

# Novel triangle method for evaluation of fracability in transitional shale: Case study from well ZXY-I in the southern North China Basin

*Energy Exploration & Exploitation*

2022, Vol. 40(3) 1036–1056

© The Author(s) 2022

DOI: 10.1177/01445987221092851

journals.sagepub.com/home/eea



Shijing Chen<sup>1,2,3</sup> , Pei Li<sup>4</sup>, Liling Qin<sup>5</sup>,  
Jinchuan Zhang<sup>1,2</sup>, Zhiguo Li<sup>6</sup> and Miao Shi<sup>7</sup>

## Abstract

Fracability is a property widely used to evaluate whether reservoirs can effectively fracture to increase production capacity. The brittleness index, which is used to evaluate reservoir fracability, is calculated via various methods, and the evaluation process of the brittleness index is complicated and not sufficiently intuitive. Thus, we used triangle method to evaluate reservoir fracability. The shale composition is classified into strong (quartz + pyrite), moderate (carbonate + plagioclase + siderite), and poor (clay + TOC + porosity) fracability based on the mechanical parameters of each shale component, which were integrated as the endpoints of the triangle method. Meanwhile, the triangle method is divided into four fracability evaluation grades: strong (I), moderate (II), weak (III) and poor (IV) fracability; each major evaluation grade has four sub-categories: best for fracturing (1), better for fracturing (2), poor for fracturing (3) and worst for fracturing (4). The triangle method is simpler and more convenient than the conventional method, dividing the fracability evaluation grades more specifically. The difference in fracability between samples can be

<sup>1</sup>Beijing Key Lab of Unconventional Natural Gas Geological Evaluation and Development Engineering, School of Energy Resources, China University of Geosciences, Beijing, China

<sup>2</sup>Key Lab of Strategy Evaluation for Shale Gas, Ministry of Natural Resources, Beijing, China

<sup>3</sup>Helmholtz Centre Potsdam, GFZ German Research Centre for Geosciences, Potsdam, Germany

<sup>4</sup>Petroleum Exploration and Production Research Institute, China Petroleum and Chemical Corporation (SINOPEC), Beijing, China

<sup>5</sup>Institute of Geology of the Second Oil Production Plant, PetroChina Huabei Oilfield Company, Hebei, China

<sup>6</sup>Bayan Project Department of the Second Oil Production Plant, PetroChina Huabei Oilfield Company, Hebei, China

<sup>7</sup>School of gemology and materials science, Hebei GEO University, Hebei, China

## Corresponding author:

Jinchuan Zhang, Beijing Key Lab of Unconventional Natural Gas Geological Evaluation and Development Engineering, School of Energy Resources, China University of Geosciences, Beijing, China.

Email: zhangjc@cugb.edu.cn



shown intuitively, which enhances the accuracy and reliability of the evaluation of transitional shales and provides theoretical support for reservoir reconstruction.

## Keywords

Fracability evaluation, novel triangle method, reservoir reconstruction, transitional shale, southern North China Basin

## Introduction

The use of unconventional oil and gas reservoirs such as shale, coal, and tight sandstone oil and gas reservoirs, can promote the energy transition from conventional to renewable energy sources (Kuchler, 2017) and achieve the carbon neutrality goal as soon as possible (Lu et al., 2021; Zhao et al., 2020). Compared with conventional reservoirs, unconventional shale, coal, and tight sandstone reservoirs, which have low porosity and ultra-low permeability, require hydraulic fracturing before the extraction of gas and oil (Javadpour, 2009; Hu et al., 2020; Lawal et al., 2021; Zhang et al., 2008). The fracability of a reservoir is typically used to describe the effects of reservoir hydraulic fracturing and reconstruction (Wang and Gale, 2009; Zhang et al., 2016). Generally, a reservoir with “better” fracability can easily form a complex fracture network and enhance the reconstruction effect (He et al., 2020; Holt et al., 2015). Therefore, the fracability evaluation of the reservoirs prior to hydraulic fracturing and reconstruction is important (Ma et al., 2019; Wu et al., 2018).

The fracability of shale reservoir largely depends on the mineralogy and mechanical properties of the reservoir, including the distribution and types of minerals, organic matter (OM), total organic carbon (TOC), porosity, and type of pores and fractures (He et al., 2020; Herrmann et al., 2019; Grieser and Bray, 2007; Lawal et al., 2021; Lora et al., 2016; Mews et al., 2019; Moghadam et al., 2019). Every type of mineral and OM in shale has a different Young's modulus and Poisson's ratio (Gholami et al., 2016; Huo et al., 2018), which can influence the fracability characteristics of the reservoir. A high Young's modulus and low Poisson's ratio suggest good reservoir fracability (Kang et al., 2020; Rickman et al., 2008). Quartz, which is a typical brittle mineral, has a high Young's modulus and low Poisson's ratio, showing good brittleness and fracability (Chen et al., 2021b). Jin et al. (2015) and Simmons and Birch (1963) illustrated that pyrite also has good fracability and is a brittle mineral, with a high Young's modulus and low Poisson's ratio. Carbonate minerals, including calcite and dolomite, have a moderate Young's modulus and Poisson's ratio, which are lower and higher than those of quartz, respectively; these minerals are non-brittle mineral and show lower fracability than quartz (Mathia et al., 2016; Mews et al., 2019). Plagioclases always are brittle mineral; however, based on their Young's modulus and Poisson's ratio, they can be classified as non-brittle (Huo et al., 2018; Woeber et al., 1963). In addition, the brittleness of siderite is higher than that of clay, but lower than that of quartz, which is a non-brittle mineral (Christensen, 1972). Clay minerals, including illite, kaolinite, chlorite, and illite-smectite mixed-layer (I-Sm) are representative ductile mineral and have poor fracability (Lawal et al., 2021; Mews et al., 2019; Moghadam et al., 2019; Yasin et al., 2017). In addition, OM exhibits ductile characteristic. However, the trend of the Young's modulus and Poisson's ratio of plagioclase is different from that of quartz and similar to that of carbonate. Plagioclase have moderate fracability and are non-brittle mineral (Huo et al., 2018; Woeber et al., 1963). The Young's modulus of siderite is higher than those of carbonate and plagioclase, which is lower than that of pyrite; the Poisson's ratio of siderite is higher than those of quartz and pyrite,

which is similar to the carbonate and plagioclase, also showing moderate fracability (Christensen, 1972). Clay minerals, including illite, kaolinite, chlorite, and I-Sm are ductile and follow the opposite trend, i.e., they have a low Young's modulus, high Poisson's ratio and show poor fracability (Lawal et al., 2021; Mews et al., 2019; Moghadam et al., 2019). In addition, OM has the lowest Young's modulus and high Poisson's ratio, which indicates worse fracability (Walles, 2004; Yasin et al., 2017).

The types of fractures and pores in shale also influence the fracability of reservoirs. Some pores and fractures between brittle minerals can be preserved during strong compaction and are connected with artificial fractures during fracturing, which is conducive to shale fracability (Chen et al., 2021b). Most pores and fractures, particularly those developed in ductile minerals, are usually closed during compaction (He and Hayatdavoudi, 2018; Oluwadebi et al., 2018; Renard et al., 2018), which is not conducive to fracability.

Fracability cannot be measured directly; therefore, many scholars use the brittleness index (BI) to quantitatively evaluate it (Hucka and Das, 1974; Kang et al., 2020; Kumar et al., 2018; Lawal et al., 2021; Rybacki et al., 2016; Tarasov and Potvin, 2013), which is defined using various calculation methods and models. There are no unified standard calculations for evaluating shale brittleness. The proportion of brittle mineral content of all minerals in shale is usually used to calculate the BI (Jarvie et al., 2007; Jin et al., 2015; Slatt and Abousleiman, 2011), such as the weight fraction of quartz (Jarvie et al., 2007; Rickman et al., 2008), the weight fraction of quartz, feldspar, carbonate and mica (Jin et al., 2015), the weight fraction of quartz and carbonate (Li et al., 2013), the weight fraction of pyrite, quartz, dolomite (Wang and Gale, 2009; Zhang et al., 2016, 2017) and even the fraction of all minerals except clay (Gale et al., 2007). The BI can also be defined using the Young's modulus and Poisson's ratio (Grieser and Bray, 2007; Kang et al., 2020; Rickman et al., 2008; Sone and Zoback, 2013), which are acquired based on the normalized and average value. Huo et al. (2018) redefined the BI by considering both the mechanical properties of different minerals and their mineral contents. Instead of the BI calculation method, a few researchers have used the triangle method to evaluate fracability and classify the evaluation grades. The triangle method is simpler and more convenient method to evaluate the fracability of shales, and the fracability grades of different shales can be compared more intuitively. Meanwhile, the accuracy and reliability of the sample fracability can be improved through a more precise division of the triangle method.

In recent years, an increasing number of unconventional oil and gas reservoirs have been discovered in the southern North China Basin (SNCB) (Chen et al., 2016; Liu et al., 2016), and the fracability of shale reservoirs must be evaluated before hydraulic fracturing. Therefore, establishing the triangle method to evaluate the fracability of transitional shale, classifying the evaluation grades of fracability and evaluating the fracability of shale in the SNCB can provide theoretical support for reservoir fracturing and exploitation.

## Samples and methods

### *Geological setting*

The southern North China Basin (SNCB), belonging to marine-continental transitional facies, is located in the southern margin of the North China Platform and covered a total area of  $15 \times 10^4 \text{ km}^2$  (Xu et al., 2003). There is a shale exploration block in SNCB which is named Wenxian shale exploration block, at the junction of Taikang Uplift and Kaifeng Depression. Compared with the multiple uplifts and reverses of strata and clockwise transgressive changes, the Wenxian shale exploration block gradually deposited Benxi-Taiyuan-Shanxi-Shihezi Formation

(Li et al., 2021). Among them, Taiyuan Formation, which developed shale, limestone, sandstone and coal seam and Shanxi Formation, which developed shale, siltstone, medium-grained sandstone and coal seam (Chen et al., 2016, 2021a; Liu et al., 2016) are the target formation (Figure 1(a)).

*Samples and methods*

The samples were collected from well ZXY-1, located at the junction of the Taikang Uplift and Kaifeng Depression in the Wenxian shale gas exploration block in the SNCB. All 14 samples were collected via cylindrical drilling, and they were marine–continental transitional shale from the Carboniferous–Permian with a depth ranging from 3260 m to 3379 m. Eight samples (Z-1–Z-8) were collected from the Shanxi Formation, and others (Z-9–Z-14) were collected from the Taiyuan Formation (Figure 1). The specific rock parameters are listed in Table 1.

In the quantitative analysis of samples, the Leco organic carbon analyzer (CS-230, China) was used to determine the TOC content, using powder samples with < 200 mesh. The BrukerD8 Discover X-ray diffractometer and composition of samples. Each sample was first crushed and samples with a particle size smaller than 10 µm was used for evaluation of total clay mineral content and non-clay mineral content, whereas others with a particle size smaller than 2 µm was used for determination of the content of each clay mineral relative to the total clay mineral content. The operation and calculation followed the relevant oil-industry standard of China (SY/T 5163-2010).

Meanwhile, Ultrapure-200A (KFSY/J95-036) was used to measure helium porosity. Samples were prepared by being processed into small cylinders with a diameter of 1 cm and subjected to drying at 105 °C for 24 h. In the qualitative analysis of the sample, FE-SEM was used for the

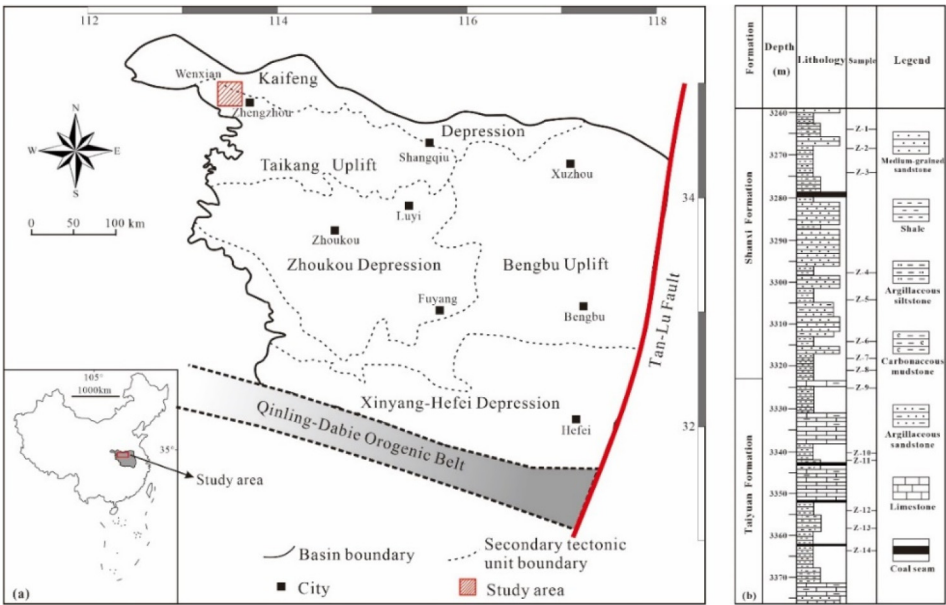


**Figure 1.** (a) Geological setting of the study area (modified after (Liu et al., 2016) and (b) the stratigraphic column and sampling locations of the lower permian Shanxi and Taiyuan formations.

Table 1. TOC content, mineral composition and porosity of Taiyuan-Shanxi shale samples.

Formation	Samples	Ro	TOC %	Quartz %	Plagioclase %	Calcite %	Dolomite %	Siderite %	Pyrite %	Clay %	Clay minerals/ %					Porosity %
											Kaolinite %	Chlorite %	Illite %	I-Sm %		
Shanxi	Z-1	4.46	0.21	33	8	1	0	0	0	58	2	7	24	67	2.43	
	Z-2	4.4	0.36	34	4	2	0	0	0	60	5	9	23	63	2.23	
	Z-3	4.32	0.8	32	8	0	0	0	0	60	6	2	17	75	2.32	
	Z-4	4.31	1.52	38	3	5	21	4	2	27	3	10	26	61	1.78	
	Z-5	4.15	4.47	34	3	2	0	2	0	59	3	9	37	51	2.21	
	Z-6	4.26	2.55	41	3	2	0	1	0	53	5	9	38	48	2.1	
	Z-7	4.24	3.27	40	3	1	1	0	1	54	0	1	29	70	1.82	
Taiyuan	Z-8	4.21	1.57	35	0	0	6	2	1	56	0	8	27	65	1.78	
	Z-9	4.2	2.44	33	4	1	0	10	3	49	2	4	19	75	1.4	
	Z-10	4.12	3.88	29	5	8	4	2	4	48	25	7	20	48	1.26	
	Z-11	4.16	2.16	57	2	6	5	0	1	29	11	3	14	72	1.8	
	Z-12	4.1	1.96	43	0	3	0	0	2	52	2	1	33	64	1.4	
	Z-13	4.09	2.35	67	1	1	0	0	3	28	4	3	29	64	1.8	
	Z-14	4.14	2.28	48	1	2	0	0	6	43	4	2	26	68	2.1	

microscopic observation of samples. The approximately  $2.5 \times 10^5 \mu\text{m}^2$  of the area of each sample were polished by the argon-ion milled (AIM) technology first and then used Hitachi SU8010 scanning electron microscope (SEM) in secondary-electron mode to identify the type and geometry of pores, fractures and minerals. For more experiments, details can see (Chen et al., 2016, 2021b).

The stress-strain experiment adopts the WEP-600 microcomputer-controlled screen display, a universal rock mechanical experimental instrument, strictly in Maccoby the recommended method of the International Society of Rock Mechanics (Rock characterization testing and monitoring-ISRM suggested method), and the samples are processed under different conditions. The maximum load-bearing capacity of the loading frame of the triaxial rock mechanics test system is 270 tons. The axial and radial displacement sensors used in the test meet the performance indicators of strain sensitivity of  $5\text{E-}6 \text{ mm/mm}$ , the accuracy of 0.2% and temperature resistance of  $200^\circ\text{C}$ . Confining pressure (simulating the horizontal stress of the formation, loading rate  $0.035 \text{ MPa/sec}$ ) and pore pressure (simulating reservoir pressure, Load rate  $0.0069 \text{ MPa/sec}$ ) and axial pressure (simulating overburden pressure, load rate  $1\text{E-}5 \text{ mm/mm/sec}$ ), and finally obtain the stress P-strain curve from deformation to failure of the rock sample, and Young's modulus and Poisson's ratio can be obtained by calculation (Diao, 2013).

## Results

### *Composition characteristics*

The TOC of the samples varied, from 0.21% to 4.47% (mean 2.05%). Clay and quartz were the main mineral components in the shale, ranging from 28% to 60% (mean 47.67%) and from 29% to 67% (mean 41.07%), respectively. The contents of plagioclase, calcite, dolomite, siderite, and pyrite were relatively low and at 0–12%, 0–8%, 0–21%, 0–10% and 0–6% respectively. Clay minerals include kaolinite, chlorite, illite, and mixed-layer of illite-smectite (I-Sm). I-Sm accounted for a large proportion, ranging from 48% to 74%. The illite content ranged between 14% and 38%. The contents of chlorite and kaolinite were lower than those of I-Sm and illite, ranging from 1% to 10% and 0% to 25%, respectively. The mineral compositions of the samples were different, which indicated that the spatial distribution of shales was strongly heterogeneous (Table 1).

### *Pore–fractures distribution*

The pore system of shales comprises inorganic and organic pores and fractures. As observed in the scanning electron microscopy (SEM) images, large inorganic pores and fractures were developed in the shales; these include shrinkage fractures, intergranular pores, intragranular and intergranular fractures, and dissolved pores (Figure 2).

Although the number of inorganic pores and fractures in the sample was large, there were also some organic pores (Figure 3(a)), intergranular fractures of OM (Figure 3(b)) and organic shrinkage fractures developed in the OM or at the edge of OM in contact with clay minerals (Figure 3). The porosity of the samples was between 1.26% and 2.43% (1.99% on average) (Table 1).

### *Key mechanical properties*

The Young's moduli of Z-9, Z-10, Z-11, Z-13, and Z-14, which belong to the Taiyuan Formation, ranged from 35.14 GPa to 36.83 GPa, whereas that of the other samples, which

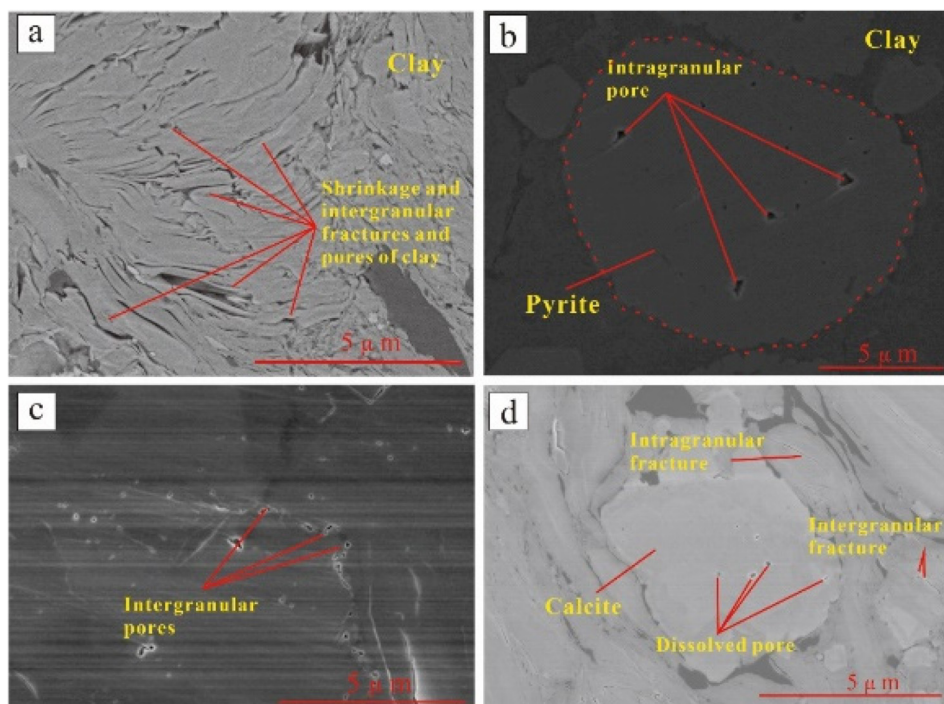


**Figure 2.** Se images of inorganic pores and fractures in the Taiyuan-Shanxi samples. (a) Shrinkage fractures of clay, Z-10, 10k, SE mode, Taiyuan Formation; (b) Intragranular pores of pyrite, Z-9, 5k, SE mode, Taiyuan Formation; (c) Intergranular pores of quartz, Z-11, 10k, SE mode, Taiyuan Formation; (d) Intragranular and intergranular fractures and dissolved pores of calcite, Z-4, 10k, SE mode, Shanxi Formation.

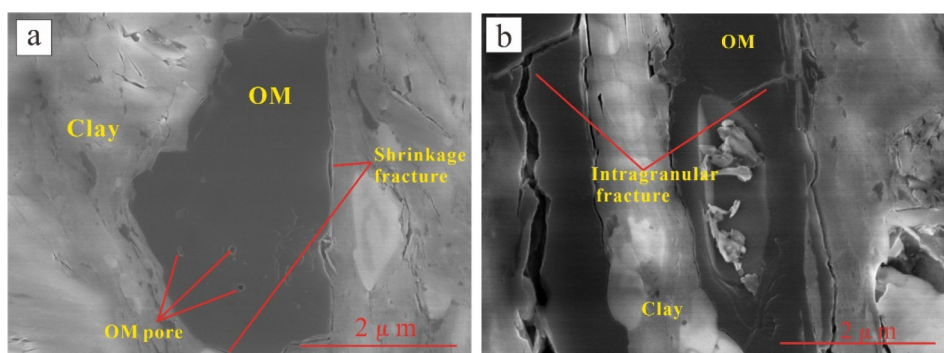


**Figure 3.** Se images of organic pores and fractures in the Taiyuan-Shanxi samples, Z-10, 20k, SE mode, Taiyuan formation. (a) Organic pores and shrinkage fractures of OM (b) Intragranular fractures of OM, Z-7, 20k, SE mode, Shanxi Formation.

belong to the Shanxi Formation, ranged from 27.5 GPa to 33.58 GPa. The Poisson's ratio of the Taiyuan and Shanxi Formation samples ranged from 0.15 to 0.16 and from 0.16 to 0.18 (Table 2).

## Discussion

### *Evaluation of triangle method*

Previous studies have focused on the calculation of the BI (Huo et al., 2018; Jin et al., 2015; Mews et al., 2019; Rickman et al., 2008; Rybacki et al., 2016; Zhang et al., 2016), discussing the BI method under different conditions and evaluating the fracability of the samples. However, a few studies have focused on using the triangle method to evaluate the fracability of samples. In this study, we established the triangle method based on the Young's modulus and Poisson's ratio for each shale composition.

The components of shales, such as minerals and OM have their own Young's modulus and Poisson's ratio, indicating that different mineral types and content influence shale fracability differently (Huo et al., 2018). As typical brittle minerals, quartz and pyrite have strong fracability (Chen et al., 2021b; Gholami et al., 2016; Jin et al., 2015; Simmons and Birch, 1963), whereas clay minerals and OM have poor fracability (Lawal et al., 2021; Mews et al., 2019; Walles, 2004; Yasin et al., 2017). Calcite, dolomite, and siderite have similar Young's moduli and Poisson's ratios, are non-brittle minerals, and contribute moderately to fracability (Mathia et al., 2016; Christensen, 1972). The plagioclase is generally classified as a brittle mineral. However, the Young's modulus and Poisson's ratio of plagioclases is different from that of quartz and similar to the that of carbonate, which demonstrates that plagioclases have moderate fracability and are non-brittle minerals (Huo et al., 2018; Woeber et al., 1963).

The types of pore-fractures and the contact types between minerals also influence the fracability of reservoirs. Under strong compaction, ductile minerals, such as OM and clay, are squeezed; and intragranular pores and cracks, shrinkage fractures of clay, and OM pores and fractures close gradually in contrast to those under concave–convex contact with adjacent particles of ductile minerals (He and Hayatdavoudi, 2018); this is not conducive to shale fracturing. Also, some intergranular and intragranular pores and fractures in quartz and dissolved pores in carbonate, positively affect the shale fracability. However, as shown in Figure 4, there is a weak positive relationship between porosity and clay, a weak negative relationship between porosity and carbonate, and no relationship between porosity and quartz, indicating that clay is the major contributor to porosity. The pores and fractures of clay are not conducive to fracturing. Meanwhile, transitional shale, especially the shale of the Shanxi and Taiyuan Formation has a higher clay content, and the average clay content is higher than that of quartz. The effect of clay on shale fracability is greater than that of quartz for clay-rich transitional shale (Han et al., 2022; Li et al., 2021). Therefore, the porosity of transitional shale will be classified as not conducive to fracturing (Oluwadebi et al., 2018; Renard et al., 2018; Yue et al., 2018).

In summary, quartz and pyrite were integrated as one endpoint of the triangle method. Carbonate, siderite, and plagioclase were integrated as another endpoint, and clay, porosity, and TOC were placed as the last endpoints of the triangle method (Figure 5). The triangle method

**Table 2.** Young's modulus and Poisson's ratio of Taiyuan-Shanxi samples.

Samples	Shanxi Formation				Taiyuan Formation				
	Z-4	Z-5	Z-6	Z-7	Z-9	Z-10	Z-11	Z-13	Z-14
Young's modulus E (GPa)	30.12	27.5	28.94	31.25	29.12	33.58	36.83	36.2	35.14
Poisson's ratio ( $\mu$ )	0.17	0.18	0.16	0.17	0.16	0.15	0.15	0.16	0.15



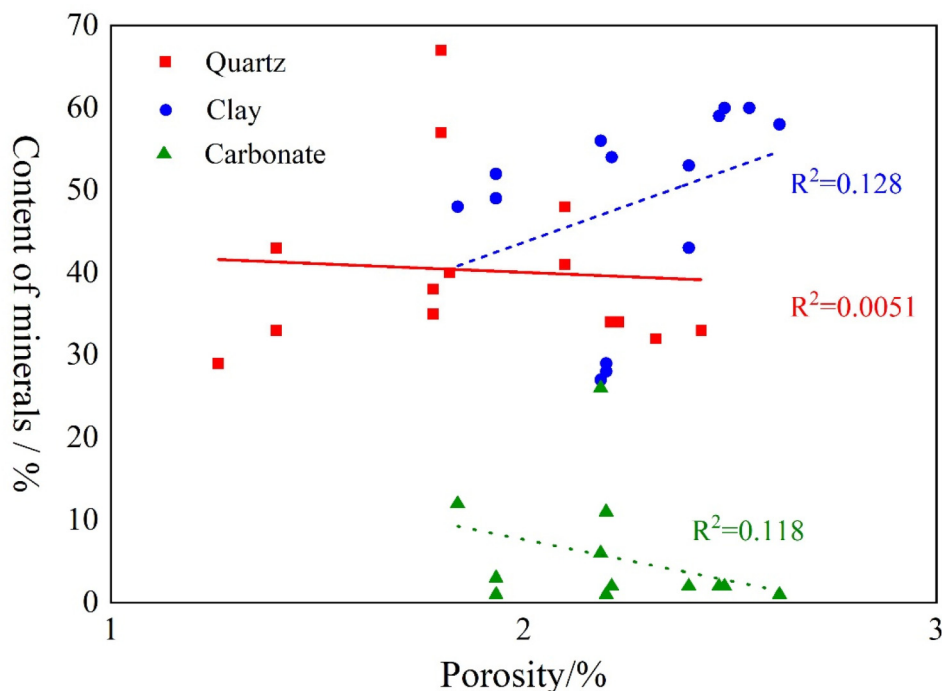


**Figure 4.** Relationship between porosity and carbonate, quartz and clay.

was divided into four levels based on the shale composition: strong (I), moderate (II), weak (III), and poor (IV) fracability. Samples with high quartz and pyrite contents have strong fracability. Samples with higher clay content, TOC content and porosity have poor fracability and samples with high carbonate, plagioclase and siderite contents have moderate fracability. To classify the grades of fracability more accurately, we divided each level into four sub-categories; best, better, poor, and worst, which facilitates the comparison of fracability in different samples.

Using the triangle method method to evaluate the fracability of shale samples from SNCB (Figure 5), it is indicated that most shale samples of the Taiyuan Formation have strong fracability and belong to grade I-4, whereas other samples belong to grade IV-1. However, most shale samples of the Shanxi Formation belong to the grade I-4, suggesting the worst fracability, and only one sample belongs to grade III-2. It is suggested that the shales fracability in the Taiyuan Formation is better than that in the Shanxi Formation, which enables complex networks and enhances the effect of reservoir reconstruction.

### Main factors controlling fracability evaluation

**Organic matter.** OM is a typical ductile material with an extremely low Young's modulus (6.2 GPa) (Carmichael, 1989; Huo et al., 2018; Mavko et al., 1998). The SEM images showed some OM filled between the mineral particles in a tortuous shape (Figure 6), revealing excellent ductility, which is not conducive to fracturing and the evaluation of fracability. As shown in Table 1, the TOC content of IV-1 shales of the Shanxi Formation has a large distribution range, ranging from 0.21% to 4.47%

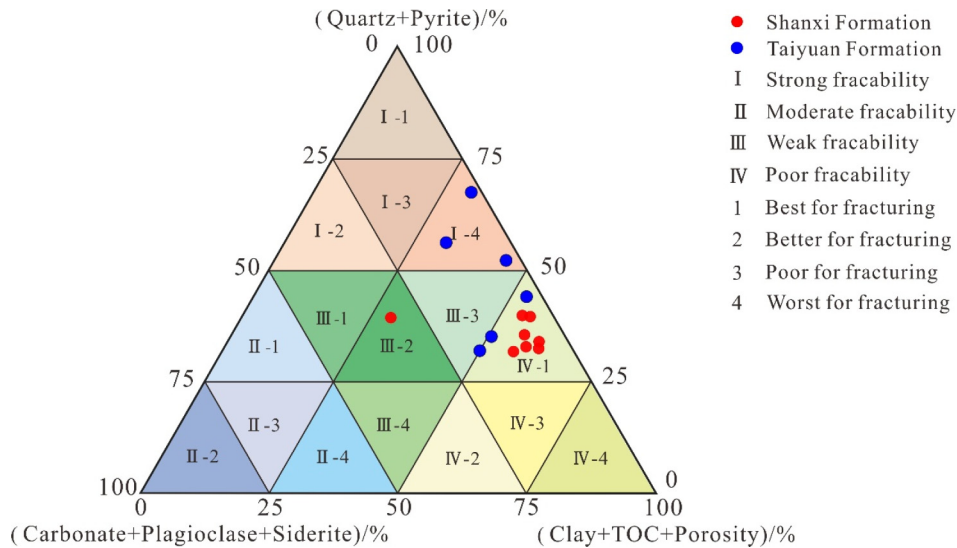


**Figure 5.** Triangle plot classification for fracability evaluation.

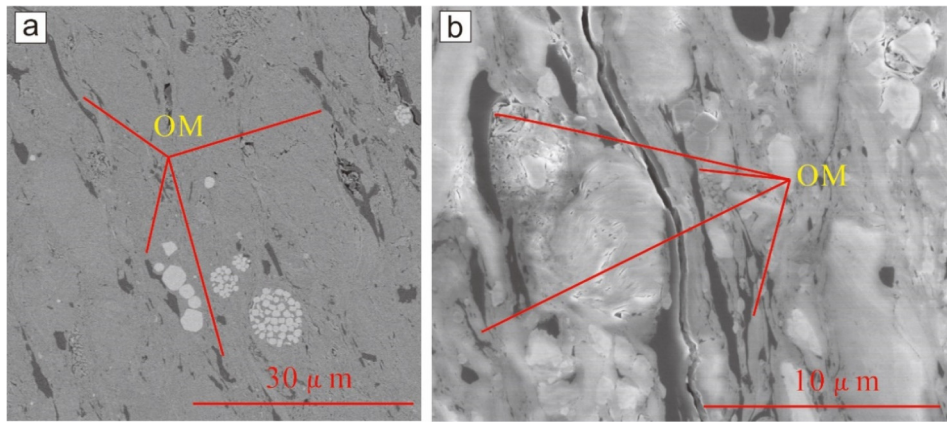


**Figure 6.** Curved organic matter of sample Z-10 in Taiyuan formation, 1.5k, SE mode (a) and sample Z-6 in Shanxi formation (b), 5k, SE mode.

(1.89% on average). The average TOC content of IV-1 shales of the Taiyuan Formation is slightly higher than that of others. However, the TOC content in the samples was very low, which contributed less to the fracability evaluation.

### Minerals

**Brittle minerals.** As a brittle mineral, quartz has a high Young's modulus and low Poisson's ratio. As shown in Figure 7(a), the quartz content of Z-11, Z-13, and Z-14, which belong to the I-4 grade, was higher than that of samples belonging to grades III-2 and IV-1. The average quartz content of I-4 samples was the highest (mean 57.34%), and it was approximately 1.64 and 1.61 times higher

than those of IV-1 shales of the Taiyuan and Shanxi Formation shales, respectively. The difference in the pyrite content was more obvious than that in quartz between I-4, III-2, and IV-1. Six shale samples from the Taiyuan Formation, which belong to grades I-4 or IV-1, had similar pyrite content, with an average of 3.33% and 3%, respectively. However, the average content of pyrite in the I-4 and IV-1 shales of the Taiyuan Formation was 11 times higher than that of IV-1 shales of the Shanxi Formation (Figure 7(b)). Therefore, the brittle mineral contents of I-4 shales were higher than those of III-2 and IV-1 shales. Concerning brittle minerals, the fracability of I-4 shales was better than that of III-2 and IV-1 shales.

**Non-brittle minerals.** Carbonate, siderite, and plagioclase are defined as non-brittle minerals based on the Young's modulus and Poisson's ratio. Although non-brittle minerals contribute less to fracturing than brittle minerals, they can also positively impact fracturing and the fracability evaluation. The carbonate content of III-2 shales was the highest, followed by those of I-4 and IV-1 shales of the Taiyuan Formation; the carbonate content of the IV-1 shales of the Shanxi Formation was the lowest. The calcite contents of I-4 shales, IV-1 shales of the Taiyuan Formation, and III-2 shales were higher than that of IV-1 shales of the Shanxi Formation (Figure 7(a)). The dolomite content of the III-2 shale was higher than that of the I-4 and IV-1 shales (Figure 8(b)).

The distribution of siderite in all shales was consistent with that of carbonate. The siderite content of IV-1 shales of the Taiyuan Formation was the highest; specifically, it was five times higher than that of IV-1 shales of the Shanxi Formation. The I-4 shales either did not contain siderite, or the siderite content was extremely low (Figure 8(c)). However, the plagioclase content showed the opposite trend. The average plagioclase content of IV-1 shales of the Shanxi Formation was the highest, and that of the I-4 shales was the lowest. The IV-1 shales of Taiyuan Formation and III-2 shale had a similar plagioclase content, which was lower than that of IV-1 shales (Figure 8(d)).

**Ductile minerals.** Clay minerals are typical ductile materials with a high Poisson's ratio (0.34) and low Young's modulus (24.1 GPa), showing poor fracturing. The IV-1 shales had the highest

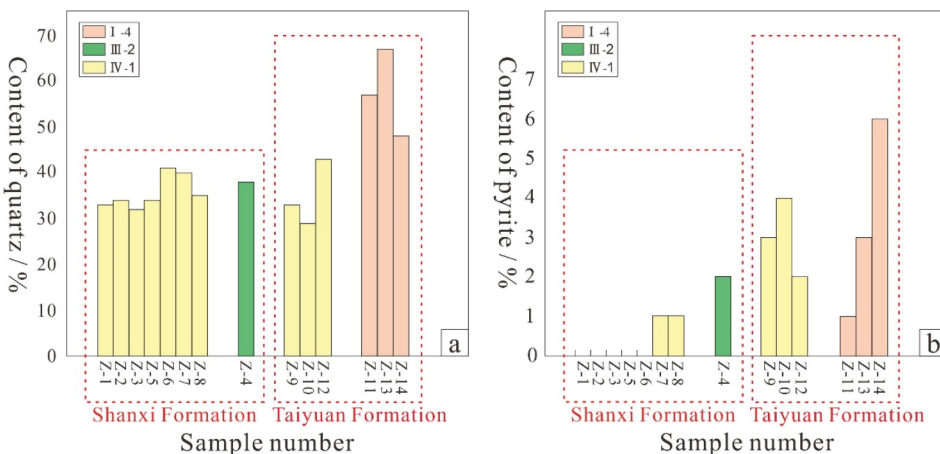


**Figure 7.** Content of quartz and pyrite in Taiyuan-Shanxi shale samples. The distribution of quartz content (a) and pyrite content (b).

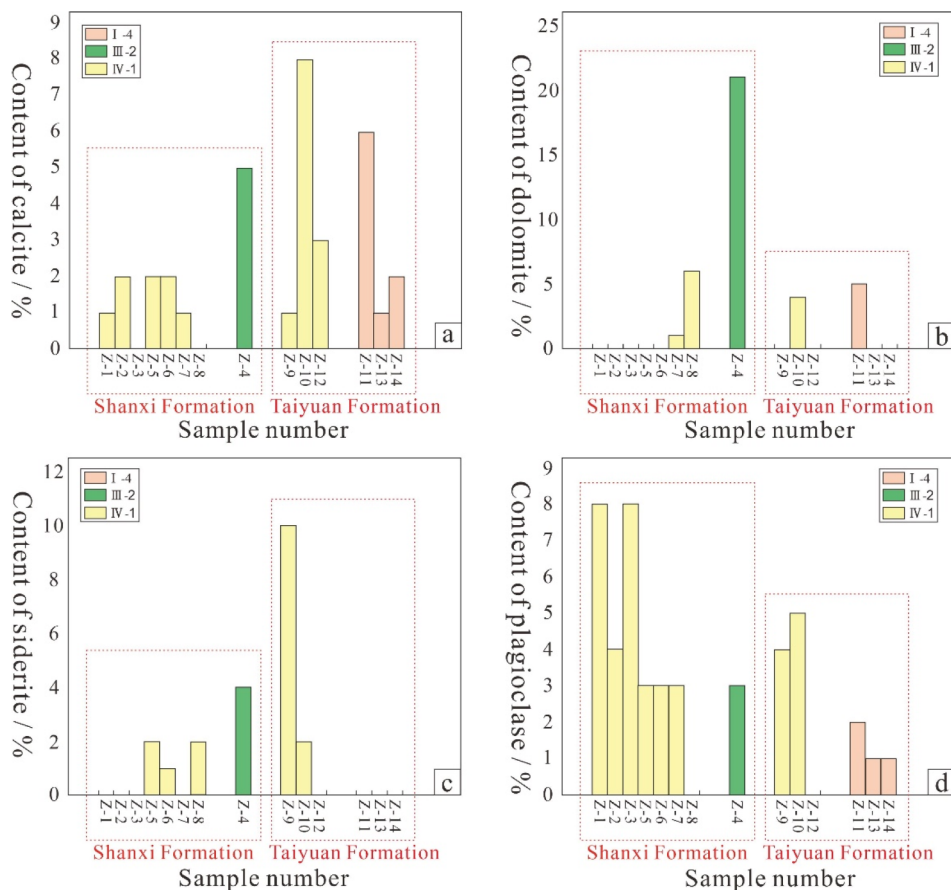


**Figure 8.** Content of non-brittle minerals in Taiyuan-Shanxi shale samples. The distribution of calcite content (a), dolomite content (b), siderite content(c), and plagioclase content (e).

clay mineral content, which was far greater than that of the other shales. The IV-1 shales of the Taiyuan Formation had a higher clay mineral content than those of the Shanxi Formation (Figure 9(a)). Clay minerals include illite, kaolinite, chlorite, and I-Sm. I-Sm has a low Young's modulus and high Poisson's ratio, indicating better ductility and poor fracability. I-4, III-2, and IV-1 had a similar I-Sm content, which accounted for the highest proportion of clay minerals (Figure 9(b)). The Young's moduli and Poisson's ratios of kaolinite and illite exhibited the same trends. As shown in Figure 9(c) and (d), the IV-1 shales of the Shanxi Formation and III-2 shale had a higher illite content than that of I-4 and IV-1 shales of the Taiyuan Formation. Also, the average kaolinite content of IV-1 shale of the Taiyuan Formation was the highest, followed by that of I-4 shale; the IV-1 samples of the Shanxi Formation and the III-2 sample had the lowest kaolinite content. Among clay minerals, chlorite has a low Poisson's ratio and high Young's modulus. The III-2 sample had a high chlorite content, followed by that of the IV-1 samples, contributing differently to sample fracturing (Figure 9(e)). The clay mineral content accounts for a large proportion of the shale composition, which can greatly influence the fracability of shale reservoirs. The higher the clay mineral content, the more unfavorable are fracturing and the fracability evaluation.

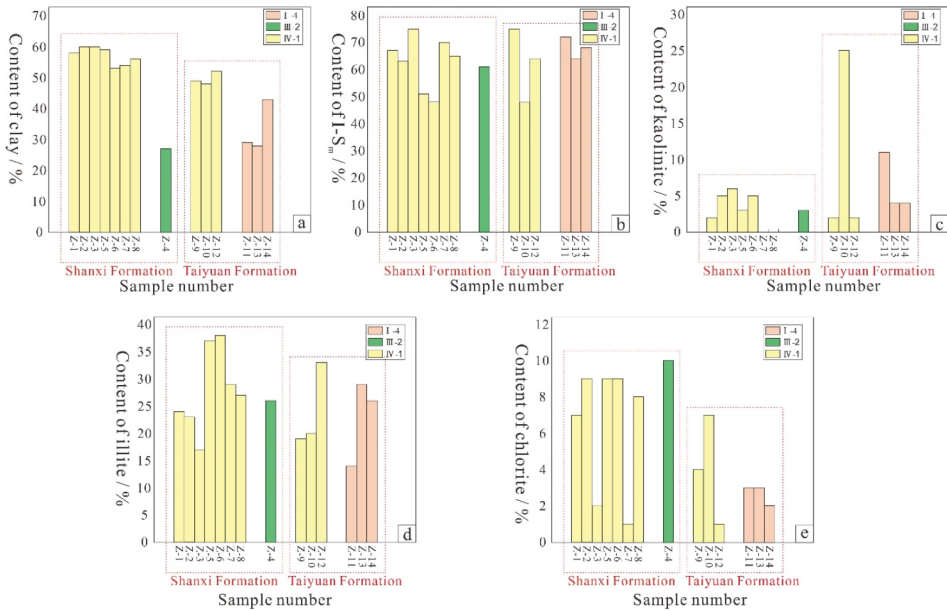


**Figure 9.** Content of different clay minerals in Taiyuan-Shanxi shale samples. The distribution of total clay content (a), I-Sm content (b), kaolinite content (c), illite content (d), and chlorite content (e).

**Pores and fractures.** The transitional shale reservoir contains many pores and fractures related to clay. However, when the reservoir is compacted, these pores and fractures are squeezed and gradually closed, which is not conducive to fracturing and fracability.

**Types of pores.** As mentioned in Section ‘Composition characteristics’, the pore types of all transitional shales include organic pores, inorganic pores, and natural fractures. Many intragranular pores and shrinkage fractures of clay develop in transitional shales (Figures 2(a), Figure 10).

Furthermore, many intragranular and shrinkage fractures of clay and OM were developed in the IV-1 shales, and a few OM pores developed in all types of shales (Figures 2(a), 3, and 9), which indicated the negative effect on shale fracability. In addition, a few intergranular pores of quartz (Figure 2(c)), intragranular pores of pyrite (Figure 2(b)), and dissolved pores of calcite (Figure 2(d)) were developed, which positively affect shale fracability to a certain extent. As mentioned in Section ‘Evaluation of triangle method’, clay is the major contributor to porosity, and its content is high; therefore, the weak effect of pores and fractures of quartz on the fracability of transitional shale can be ignored.

**Porosity.** The intergranular pores and intercrystalline cracks of clay and intercrystalline pores of pyrite were the main contributors to porosity. When the reservoir is squeezed by compaction, ductile minerals, such as clay, deform, and related pores and fractures are closed; this reduces the effect of reconstruction during fracturing. The average porosities of I-4 shales, IV-1 shales of the Shanxi Formation, and III-2 shales were similar at 1.9%, 2.12%, and 1.78%, respectively. The IV-1 shale of the Taiyuan Formation had a lower porosity of 1.35% (Figure 11). The difference in the porosity of all samples was small, which implied that the porosity of transitional shales is not a major factor in the evaluation of fracability.



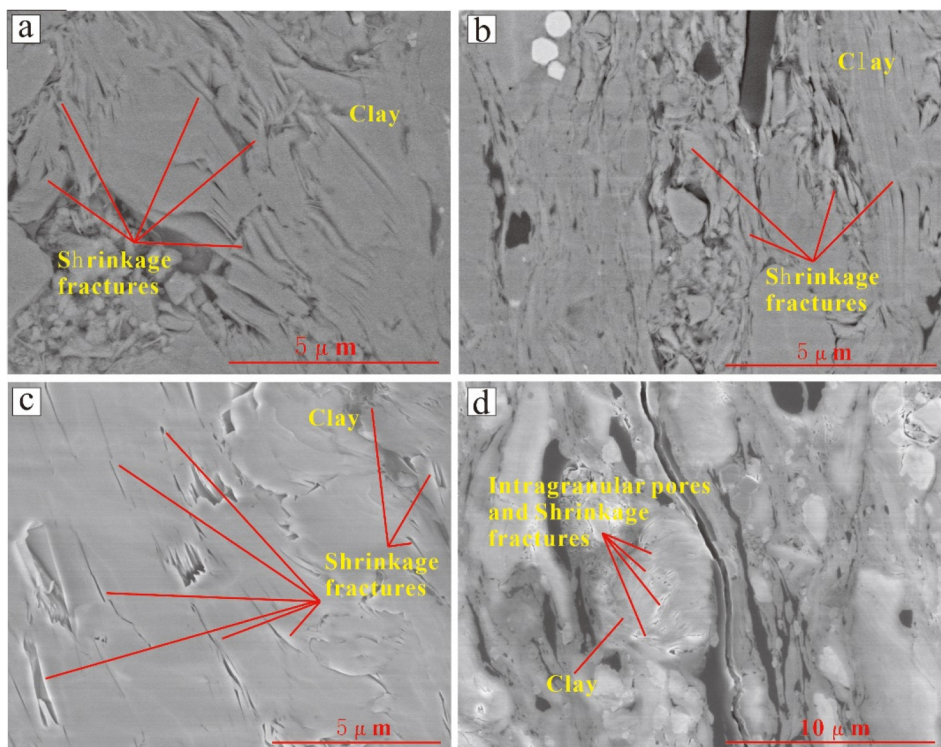


**Figure 10.** Se images of shrinkage fractures and pores of the clay in Taiyuan-Shanxi samples. (a) Shrinkage fractures in clay minerals, Z-3, 10k, SE mode, Shanxi Formation; (b) Shrinkage fractures in clay minerals, Z-5, 10k, SE mode, Shanxi Formation; (c) Along with bedding shrinkage fractures of shales, Z-9, 20k, SE mode, Taiyuan Formation; (d) Intragranular pores and shrinkage fractures in clay minerals, Z-6, 5k, SE mode, Shanxi Formation.

**Young's modulus and Poisson's ratio.** The Young's modulus and Poisson's ratio can reflect the mechanical properties of the shales, which can be used to evaluate fracability. The Young's modulus and Poisson's ratio of all I-4 shales of the Taiyuan Formation were greater than 35 GPa and lower than 0.16, respectively (Figure 12), which indicated 'better' fracability. However, the IV-1 shales of the Shanxi Formation showed the opposite trend, with the lowest average Young's modulus (29.23 GPa) and the highest Poisson's ratio (0.17), showing the worst fracability. IV-1 shales of Taiyuan Formation and III-2 shales had a moderate Young's modulus and Poisson's ratio, showing moderate fracability.

The Young's modulus of shales from the Taiyuan Formation (35.14–36.83 GPa) was greater than that of the Shanxi Formation (27.5–33.58 GPa). However, the Poisson's ratio of the Taiyuan Formation shales ranged from 0.15 to 0.16, which was lower than that of the Shanxi Formation (0.16–0.18).

### **Fracability evaluation of transitional shale**

**Fracability evaluation of transitional shale by the triangle method.** The IV-1 included shale of the Taiyuan and Shanxi Formations (Figure 5). Sample Z12, which was collected from the Taiyuan

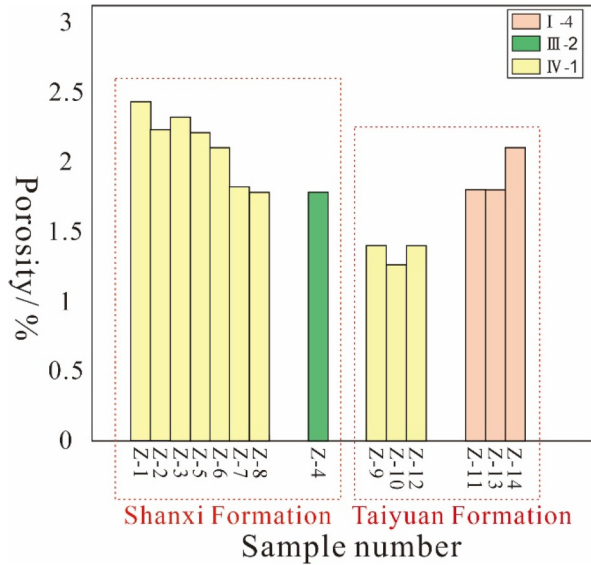


**Figure 11.** Porosity distribution of Taiyuan-Shanxi shales.

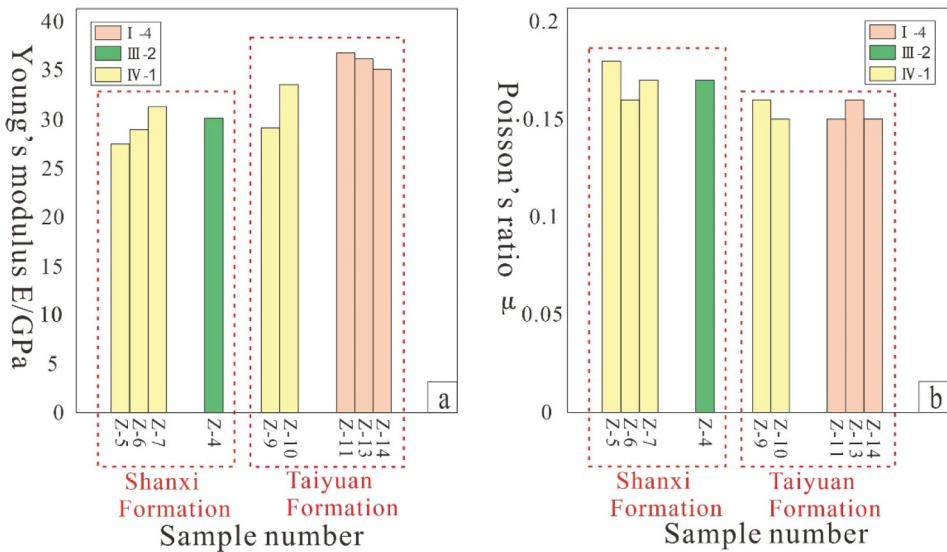


**Figure 12.** Young's modulus (a) and Poisson's ratio (b) of Taiyuan-Shanxi shale samples.

Formation, had the highest quartz and pyrite contents in IV-1 and lower clay content, TOC content, and porosity than other shales collected from the Shanxi Formation, showing 'better' fracability. The Z9 and Z10 samples collected from the Taiyuan Formation had a similar quartz content with that of most IV-1 samples collected from the Shanxi Formation; however, they had a lower clay content, TOC content, and porosity and higher carbonate, plagioclase, and siderite contents than most IV-1 samples collected from the Shanxi Formation. Meanwhile, all I-4 shales were

collected from the Taiyuan Formation. Therefore, based on the triangle method, the fracability of the Taiyuan Formation was better than that of the Shanxi Formation.

Quartz and clay are the main components of shale (Table 1), and they significantly affected fracability. Quartz, a brittle mineral, can improve fracability, whereas clay, which is a ductile mineral, negatively affects it. As shown in Figure 13(a), the shales of the Taiyuan Formation had the highest quartz content and the lowest clay content, and they showed the best fracability. However, the shales of the Shanxi Formation showed the opposite trend with poor fracability. After normalizing the illite, kaolinite, chlorite, and I-Sm contents, we found that the contents of I-Sm and illite of the Shanxi Formation were higher than those of the Taiyuan Formation. I-Sm and illite are typical ductile minerals and are moderately present in shale; thus, they have a negligible effect on fracability evaluation.

The other components of shale do not contribute significantly to reservoir fracability, but they can still affect the fracability evaluation. The contents of calcite, siderite, and pyrite in the shale of the Taiyuan Formation were higher than those of the Shanxi Formation. Calcite and siderite are non-brittle minerals, whereas pyrite is brittle. The pyrite content of the Taiyuan Formation shale was six times that of the Shanxi Formation shale, which made the Taiyuan Formation shale more fracable. The TOC and kaolinite contents of the Taiyuan Formation shale were slightly higher than those of the Shanxi Formation shale; however, the content and difference were small, and the impact can be ignored. The dolomite and plagioclase contents and porosity of the Shanxi Formation were slightly higher than those of the Taiyuan Formation shale (Figure 13(b)). Because clay has a greater influence on the fracability evaluation, the fracability of the Shanxi Formation shale was poorer than that of the Taiyuan Formation shale, which is mainly influenced by the quartz and clay contents.

**Comparison with the conventional method.** There is no unified standard method for the evaluation of shale brittleness; the BI is used to evaluate shale brittleness and fracability based on the mineral composition or mechanical parameters. The BI can usually be calculated using the Young's modulus and Poisson's ratio, brittle mineral content, and mechanical properties of different minerals and their mineral content. Three methods were used to calculate the BIs of all samples. The BIs of the Taiyuan Formation samples were mostly greater than those of the Shanxi Formation

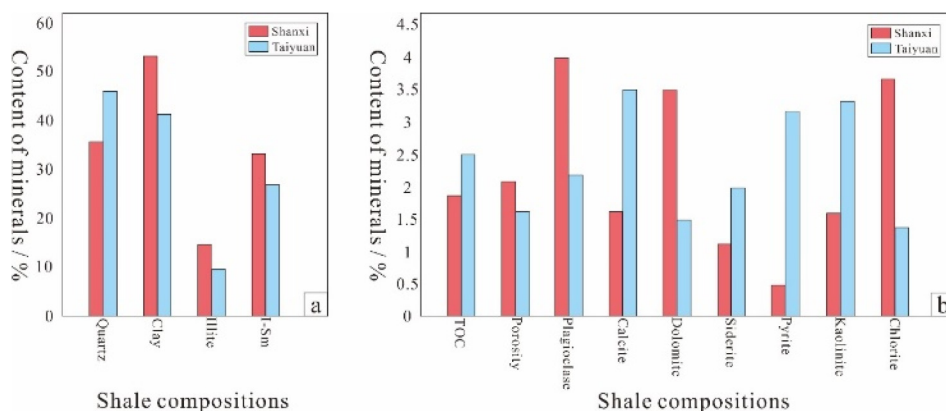


**Figure 13.** Compositions of Taiyuan-Shanxi shale samples. (a) The content of quartz, clay, illite and I-Sm; (b) The content of plagioclase, calcite, dolomite, siderite, pyrite, kaolinite and chlorite, and TOC and porosity.



**Table 3.** The BI and fracability evaluation results of Taiyuan-Shanxi shales based on the different methods.

Sample	BI			Triangle method classification	Fracability evaluation of formation
	Mineral composition	Mechanical parameter	Mechanical parameter and mineral composition		
Shanxi Formation	Z-1	0.36	/	0.37	Poor fracability
	Z-2	0.35	/	0.37	
	Z-3	0.35	/	0.35	
	Z-4	0.41	0.59	0.49	
	Z-5	0.36	0.5	0.37	
	Z-6	0.43	0.19	0.44	
	Z-7	0.42	0.25	0.45	
	Z-8	0.36	/	0.41	
Taiyuan Formation	Z-9	0.40	0.5	0.42	Better fracability
	Z-10	0.33	0.29	0.40	
	Z-11	0.59	0.5	0.62	
	Z-12	0.44	/	0.48	
	Z-13	0.70	0.96	0.72	
	Z-14	0.52	0.39	0.58	

(Table 3). Rickman et al. (2008) stated that the critical value of the BI for evaluating the fracability of samples is 0.4. When the BI is greater than 0.4, the sample is conducive to fracturing and forming a complex network, which has better fracability. Meanwhile, if the BI of the sample is greater than 0.6, there is higher brittleness and the best fracability. The BI of the Taiyuan Formation shales was mostly higher than 0.4 and even higher than 0.6 in some samples; however, the BI of most samples of the Shanxi Formation was lower than 0.4. Therefore, the shale fracability of the Taiyuan Formation was better than that of the Shanxi Formation.

According to the above analysis, the fracability evaluation results of the triangle and conventional methods are consistent (Table 3), which proves the accuracy and reliability of the triangle method. Furthermore, the triangle method is simpler and more reasonable and effective than the conventional evaluation methods. The fracability of different samples and the difference in fracability between samples can be shown intuitively. The triangle method divides the fracability evaluation grades of shales more specifically, which enhances the accuracy and reliability of the fracability evaluation and provides theoretical support for reservoir reconstruction. In the future, it would be valuable to examine rock brittleness and fracability in other areas.

## Conclusion

1. We established a novel triangle method for evaluating fracability. The shale composition was separated into best fracability and mechanically strong (quartz + pyrite), moderate fracability (carbonate + plagioclase + siderite), and poor fracability (clay + TOC + porosity). Mineral data are given in vol% and normalized to 100 vol%, considering the TOC content and porosity of the shale samples.

2. The triangle method was divided into four fracability evaluation grades: strong (I), moderate (II), weak (III), and poor (IV) fracability. Each fracability evaluation grade was evenly divided into four secondary evaluation grades: best (1), better (2), poor (3), and worst (4) for fracturing.
3. The triangle method for evaluating fracability is simpler and more reasonable and effective than the conventional method. The fracability of different samples and the difference in fracability between samples can be shown intuitively. In addition, the triangle method divides the fracability evaluation grades of shales more specifically, which enhances the accuracy and reliability of the evaluation and provides theoretical support for reservoir reconstruction.
4. The fracability of shales collected in the Taiyuan Formation from the SNCB was greater than that of the shales collected in the Shanxi Formation, which indicates that the Taiyuan Formation is more conducive to fracturing, forming a complex network, and enhancing the effect of reservoir reconstruction.

## Highlights

1. A novel triangle method was established to evaluate the shale fracability.
2. The triangle method was divided into four fracability evaluation grades: strong (I), moderate (II), weak (III), and poor (IV) fracability.
3. Each fracability evaluation grade was evenly divided into four secondary evaluation grades: best (1), better (2), poor (3), and worst (4) for fracturing.
4. The triangle method for evaluating fracability is simpler and more reasonable and effective than the conventional method

## Acknowledgements

This work was jointly supported by the National Natural Science Foundation of China (Grant No. 41927801); the National Science and Technology Major Project (Grant No. 2016ZX05034002-001); the 2021 Graduate Innovation Fund Project of China University of Geosciences, Beijing (Grant No. ZD2021YC025); National Natural Science Foundation of China (Grant No. 42002156); Natural Science Foundation of Hebei Province of China (Grant No. D2021403015).


## Declaration of conflicting interests

The author(s) declared no potential conflicts of interest with respect to the research, authorship, and/or publication of this article.

## Funding

The author(s) disclosed receipt of the following financial support for the research, authorship, and/or publication of this article: This work was supported by National Natural Science Foundation of China, the National Science and Technology Major Project, the 2021 Graduate Innovation Fund Project of China University of Geosciences, Beijing, National Natural Science Foundation of China and Natural Science Foundation of Hebei Province of China, (grant number Grant No. 41927801, Grant No. 2016ZX05034002-001, Grant No. ZD2021YC025, Grant No. 42002156, Grant No. D2021403015).

## ORCID iD

Shijing Chen  <https://orcid.org/0000-0002-7210-4285>

## References

- Carmichael RS (1989) *Practical Handbook of Physical Properties of Rocks and Minerals*. CRC Press, Boca Raton, Florida, p. 741.
- Chen Q, Zhang JC, Tang X, et al. (2016) Pore structure characterization of the lower permian marine-continental transitional black shale in the Southern North China Basin, Central China. *Energy & Fuels* 30(12): 10092–10105.
- Chen SJ, Li P, Zhang JC, et al. (2021a) Measurement of shale wettability using calorimetry: experimental results and model. *Energy & Fuels* 35(21): 17446–17462.
- Chen SJ, Liu Y, Zhang JC, et al. (2021b) Formation conditions and evolution of fractures in multiple tight rocks: implications for unconventional reservoir exploitation. *Journal of Petroleum Science and Engineering* 200: 108354.
- Christensen NI (1972) Elastic properties of polycrystalline magnesium, iron, and manganese carbonates to 10 kilobars. *Journal of Geophysical Research* 77(2): 369–372.
- Diao HY (2013) Rock mechanical properties and brittleness evaluation of shale reservoir. *Acta Petrologica Sinica* 29(9): 3300–3306 (in Chinese with English abstract).
- Gale JFW, Reed RM and Holder J (2007) Natural fractures in the Barnett Shale and their importance for hydraulic fracture treatments. *AAPG Bulletin* 91(4): 603–622.
- Gholami R, Rasouli V and Sarmadivaleh M (2016) Brittleness of gas shale reservoirs: A case study from the north Perth basin, Australia. *Journal of Natural Gas Science and Engineering* 33: 1244–1259.
- Grieser WV and Bray JM (2007) Identification of production potential in unconventional reservoirs. In: SPE Production and Operations Symposium, Oklahoma City, USA
- Han M, Wie XL, Zhang J, et al. (2022) Influence of structural damage on evaluation of microscopic pore structure in marine continental transitional shale of the Southern North China Basin: A method based on the low-temperature N<sub>2</sub> adsorption experiment. *Petroleum Science* 19(1): 100–115.
- He WH and Hayatdavoudi A (2018) A comprehensive analysis of fracture initiation and propagation in sandstones based on micro-level observation and digital imaging correlation. *Journal of Petroleum Science and Engineering* 164: 75–86.
- He JM, Li X, Yin C, et al. (2020) Propagation and characterization of the micro-cracks induced by hydraulic fracturing in shale. *Energy* 191(15): 116449.
- Herrmann J, Rybacki E and Sone H (2019) Deformation experiments on bowland and posidonia shale – part II: creep behavior at in situ pc–T conditions. *Rock Mechanics and Rock Engineering* 53(2): 755–779.
- Holt RM, Fjær E, Stenebråten JF, et al. (2015) Brittleness of shales: relevance to borehole collapse and hydraulic fracturing. *Journal of Petroleum Science and Engineering* 131: 200–209.
- Hu Q, Liu L, Li Q, et al. (2020) Experimental investigation on crack competitive extension during hydraulic fracturing in coal measures strata. *Fuel* 265: 117003.
- Hucka V and Das B (1974) Brittleness determination of rock by different methods. *International Journal of Rock Mechanics and Mining Sciences & Geomechanics Abstracts* 11(10): 389–392.
- Huo ZP, Zhang JC, Li P, et al. (2018) An improved evaluation method for the brittleness index of shale and its application – A case study from the southern north China basin. *Journal of Natural Gas Science and Engineering* 59: 47–55.
- Jarvie DM, Hill RJ, Ruble TE, et al. (2007) Unconventional shale-gas systems: the Mississippian Barnett Shale of north-central Texas as one model for thermogenic shale-gas assessment. *AAPG Bulletin* 91(4): 475–499.
- Javadpour F (2009) Nanopores and apparent permeability of gas flow in mudrocks (shales and siltstone). *Petroleum Society of Canada* 48(8): 16–21.
- Jin XC, Shah SNR, Jean-Claude R, et al. (2015) An integrated petrophysics and geomechanics approach for fracability evaluation in shale reservoirs. *Society of Petroleum Engineers SPE Journal* 20(03): 518–526.
- Kang YS, Shang CJ, Zhou H, et al. (2020). Mineralogical brittleness index as a function of weighting brittle minerals – from laboratory tests to case study. *Journal of Natural Gas Science and Engineering* 77:103278.
- Kuchler M (2017) Post-conventional energy futures: rendering Europe's shale gas resources governable. *Energy Research & Social Science* 31: 32–40.

- Kumar S, Das S, Bastia R, et al. (2018) Mineralogical and morphological characterization of older cambay shale from North Cambay Basin, India: implication for shale oil/gas development. *Marine and Petroleum Geology* 97: 339–354.
- Lawal LO, Mahmoud M, Adebayo A, et al. (2021) Brittleness and microcracks: A new approach of brittleness characterization for shale fracking. *Journal of Natural Gas Science and Engineering* 87: 103793.
- Li J, Han SD and Zhao Y (2013) Kernel density feature based improved chan-veise model for image segmentation. *6th International Congress on Image and Signal Processing (CISP)* 31(4): 616–620.
- Li P, Zhang JC, Rezaee R, et al. (2021) Effect of adsorbed moisture on the pore size distribution of transitional shales: insights from clay swelling and lithofacies difference. *Applied Clay Science* 201: 105926.
- Liu Y, Zhang JC and Tang X (2016) Predicting the proportion of free and adsorbed gas by isotopic geochemical data: A case study from lower permian shale in the southern North China basin (SNCB). *International Journal of Coal Geology* 156: 25–35.
- Lora RV, Ghazanfari E and Izquierdo EA (2016) Geomechanical characterization of Marcellus Shale. *Rock Mechanics and Rock Engineering* 49(9): 3403–3424.
- Lu YY, Zhou JP, Xian XF, et al. (2021) Research progress and prospect of the integrated supercritical CO<sub>2</sub> enhanced shale gas recovery and geological sequestration. *Natural Gas Industry* 6: 60–73.
- Ma C, Dong C, Lin C, et al. (2019) Influencing factors and fracability of lacustrine shale oil reservoirs. *Marine and Petroleum Geology* 110: 463–471.
- Mathia E, Ratcliffe K and Wright M (2016) Brittleness Index-A parameter to embrace or avoid? Unconventional Resources Technology Conference, San Antonio, Texas, 1–3 August Society of Exploration Geophysicists, American Association of Petroleum Geologists, Society of Petroleum Engineers, pp. 1156–1165.
- Mavko G, Mukerji T and Dvorkin J (1998) *The Rock Physics Handbook: Tools for Seismic Analysis of Porous media*. University of Cambridge.
- Mews KS, Alhubail MM and Barati RG (2019) A review of brittleness index correlations for unconventional tight and ultra-tight reservoirs. *Geosciences* 9(7): 319.
- Moghadam A, Harris NB, Ayranci K, et al. (2019) Brittleness in the Devonian Horn River shale, British Columbia, Canada. *Journal of Natural Gas Science and Engineering* 62: 247–258.
- Oluwadebi AG, Taylor KG and Dowe PJ (2018) Diagenetic controls on the reservoir quality of the tight gas collyhurst sandstone formation, lower permian, East Irish Sea Basin, United Kingdom. *Sedimentary Geology* 371: 55–74.
- Renard F, Weiss J, Mathiesen J, et al. (2018) Critical evolution of damage toward system-size failure in crystalline rock. *Journal of Geophysical Research: Solid Earth* 123(2): 1969–1986.
- Rickman R, Mullen MJ, Petre JE, et al. (2008) A practical use of shale petrophysics for stimulation design optimization: all shale plays are of not clones the Barnett Shale. In: SPE paper 115258, Proceedings of the Society of Petroleum Engineers (SPE) Annual Technical Conference and Exhibition.
- Rybacki E, Meier T and Dresen G (2016) What controls the mechanical properties of shale rocks? – part II: brittleness. *Journal of Petroleum Science and Engineering* 144: 39–58.
- Simmons G and Birch F (1963) Elastic constants of pyrite. *Journal of Applied Physics* 34(9): 2736–2738.
- Slatt RM and Abousleiman Y (2011) Merging sequence stratigraphy and geomechanics for unconventional gas shales. *The Leading Edge* 30(3): 274–282.
- Sone H and Zoback MD (2013) Mechanical properties of shale-gas reservoir rocks – part 2: ductile creep, brittle strength, and their relation to the elastic modulus. *Geophysics* 78(5): D393–D402.
- Tarasov B and Potvin Y (2013) Universal criteria for rock brittleness estimation under triaxial compression. *International Journal of Rock Mechanics and Mining Sciences* 59: 57–69.
- Walls F (2004) A new method to help identify unconventional targets for exploration and development through integrative analysis of clastic rock property field. *Houston Geological Society Bulletin* 47(2): 35–49.
- Wang FP and Gale JFW (2009) Screening criteria for shale-gas systems. *The Gulf Coast Association of Geological Societies Transactions* 59: 779–793.

- Woeber AF, Katz S and Ahrens TJ (1963) Elasticity of selected rocks and minerals. *Geophysics* 28(4): 658–663.
- Wu JJ, Zhang SH and Cao H (2018) Fracability evaluation of shale gas reservoir: A case study in the lower Cambrian niutitang formation, northwestern Hunan, China. *Journal of Petroleum Science and Engineering* 164: 675–684.
- Xu HL, Zhao ZJ, Yang YN, et al. (2003) Structural pattern and structural style of the southern North China Basin. *ACTA Geoscientia Sinica* 24(1): 27–33.
- Yasin Q, Du QZ, Sohail GM, et al. (2017) Impact of organic contents and brittleness indices to differentiate the brittle-ductile transitional zone in shale gas reservoir. *Geosciences Journal* 21(5): 779–789.
- Yue DL, Wu SH, Xu ZY, et al. (2018) Reservoir quality, natural fractures, and gas productivity of upper triassic Xujiahe tight gas sandstones in western Sichuan Basin, China. *Marine and Petroleum Geology* 89(2): 370–386.
- Zhang CC, Dong DZ, Wang Y, et al. (2017) Brittleness evaluation of the upper ordovician wufeng–lower silurian longmaxi shale in Southern Sichuan Basin, China. *Energy Exploration & Exploitation* 35(4): 430–443.
- Zhang DC, Ranjith PG and Perera MSA (2016) The brittleness indices used in rock mechanics and their application in shale hydraulic fracturing: A review. *Journal of Petroleum Science and Engineering* 143: 158–170.
- Zhang JC, Xu B, Nie HK, et al. (2008) Exploration potential of shale gas resources in China. *Natural Gas Industry* 28(6): 136–140.
- Zhao WZ, Jia AI, Wei YS, et al. (2020) Progress in shale gas exploration in China and prospects for future development. *China Petroleum Exploration* 25(01): 31–44.